BIOCHEMISTRY
including biophysical chemistry & molecular biology
Rapid Report

Biochemistry **2010,** *49,* 5829–5831 5829
DOI: 10.1021/bi1007436

Rational Manipulation of Amyloidogenesis Using an Atomic Level Map of Peptide−Fibril Interactions†

Yanfang Liang,‡ Shohreh Zahedi Jasbi,‡ Sylvie Morin,‡ and Derek J. Wilson*,‡,§

‡*Department of Chemistry, York University, Toronto, Ontario M3J 1P6, Canada, and* §*Center for Research in Biomolecular Interactions, Toronto, Ontario M3J 1P6, Canada*

Received May 11, 2010; Revised Manuscript Received June 17, 2010

ABSTRACT: Amyloidogenic aggregation has been the subject of intense research over the past few decades, but the mechanisms underlying the early stages of amyloidogenesis remain elusive. Here we demonstrate for the first time manipulation of amyloidogenesis based on an atomic level map of peptide−fibril interactions in early- and late-stage ordered aggregation. Several point mutants with specific amyloidogenic properties are introduced, including one that "stalls" early in the aggregation process, forming early-stage fibrillar aggregates, but not mature fibrils.

Amyloidosis is a pathogenic form of protein aggregation that has been the subject of intensive research since being linked to several common human neurodegenerative diseases in the early 1980s (*1*). These efforts have yielded a number of important insights (*2*−*5*), among which is the observation that, while a hallmark of neurodegenerative disease, fully developed amyloid plaques are not in themselves strongly neurotoxic (*6*). Mixtures containing pre-amyloid oligomers, on the other hand, are highly cytotoxic, suggesting that cell death may result from an as yet unidentified common amyloid precursor (*7*, *8*). This has led to growing interest in the early stages of ordered aggregation in recent years (*9*−*11*); however, the detailed mechanisms underlying early-stage amyloidogenesis remain poorly understood.

We have recently acquired an atomic level map of peptide−fibril interactions in early- and late-stage amyloidogenesis of a transthyretin peptide, $TTR_{(105-115)}$, using saturation transfer NMR spectroscopy (STD NMR) (*12*). In this work, these data provide a rationale for generating, on the first attempt, a point mutant that undergoes early-stage ordered aggregation but does not progress to mature fibrils. To the best of our knowledge, this is the first manipulation of amyloidogenesis based on mechanistic experimental data, and the resultant species is the first known to stall (without intervention) in the earliest phase of fibrillar aggregation.

Transthyretin, a carrier of retinol and thyroxine in plasma, is the most common hereditary systemic amyloidosis (*13*). Amyloidogenic propensity in human TTR is promoted by an 11-residue peptide, $TTR_{(105-115)}$ (Y-T-I-A-A-L-L-S-P-Y-S), which readily forms amyloid-like aggregates in vitro and is therefore a convenient model for amyloidogenic aggregation (*14*). FRET and ssNMR evidence indicates that the smallest observable fibrillar aggregates of $TTR_{(105-115)}$, protofibrils, consist of β-sheets composed of "in register" parallel strands (*15*, *16*). Protofilaments are composed of four protofibrils wound together in an antiparallel arrangement (*15*). Stacking of $TTR_{(105-115)}$ strands within protofilaments is slightly offset (1−3°) in the plane perpendicular to the fibril axis (*15*), generating a periodic twist that can be observed by atomic force microscopy (AFM) (*17*) and transmission electron microscopy (TEM) (*16*). Mature fibrils consist of approximately four intertwined protofilaments (*15*, *17*).

While $TTR_{(105-115)}$ is exceptionally well characterized as an amyloidogenic species, including high-resolution "in fibril" peptide structures (*15*) and computational models of early oligomerization (*18*), there are few experimental data to provide details about the mechanism of ordered aggregation. Using STD NMR, we acquired evidence that $TTR_{(105-115)}$ amyloidogenesis occurs in at least two distinct phases, each governed by different peptide−fibril interactions (*12*). A depiction of the interactions is provided in Scheme 1.

Scheme 1: Crucial Peptide−Fibril Interactions As Indicated by the Proximity of Specific Protons on Binding

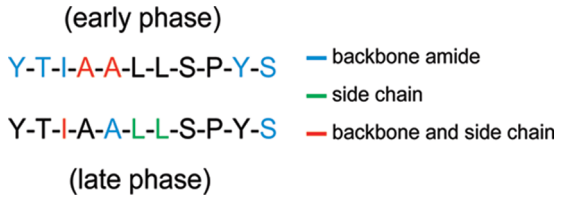

These results support the notion that, even for peptide models in which there is good reason to expect a straightforward "assembly of monomers" mechanism, the process from protofibril formation to elongation of mature fibrils is complex and multiphase. A multiphase mechanism also implies that it may be possible to selectively disrupt interactions that are crucial for the incorporation of soluble $TTR_{(105-115)}$ into mature fibrils without affecting interactions associated with the formation of prefibrilar aggregates and protofibrils. To test this hypothesis, we generated the set of point mutants shown in Scheme 2.

Mutant 1 was designed with the aim of disrupting side chain interactions at Leu_{110}, which appear to be important mainly in late-phase aggregation (see Scheme 1). The replacement residue, Asp, was selected for its similarly sized side chain with the opposite (i.e., polar) functionality, in order to favor specific chemical (rather than physical) on the soluble species. We are in most cases unable to identify the interacting group on the fibril. However, because of the central position of Leu_{110} in the sequence, and assuming in register stacking, we can hypothesize that the wild-type interaction is with Leu_{110} on an adjacent sheet. Thus, we predict that mutant 1 will exhibit weakened sheet−sheet

†This work was supported by the Canadian Foundation for Innovation (Project 12923).
*To whom correspondence should be addressed. Phone: (416) 736-2100, ext. 20786. Fax: (416) 736-5936. E-mail: dkwilson@yorku.ca.

Published on Web 06/18/2010

Scheme 2: $TTR_{(105-115)}$ Point Mutants Designed To Exhibit Specific Amyloidogenic Behaviors (for additional mutants tested, see Scheme S1)

(1) Y-T-I-A-A-D-L-S-P-Y-S disrupt late-phase only

(2) Y-T-S-A-A-L-L-S-P-Y-S disrupt both phases

(3) Y-T-I-A-A-L-L-R-P-Y-S disrupt neither phase

interactions, reducing or preventing the formation of aggregates that require sheet-to-sheet stacking (i.e., protofilaments and mature fibrils).

In mutant 2, where the aim is to completely and nonspecifically disrupt ordered aggregation, we replace the bulky, nonpolar side chain of Ile_{107} with a small, polar side chain. Because Ile_{107} appears to play a crucial role in both early- and late-stage ordered aggregation (see Scheme 1), this mutant should not form ordered aggregates of any kind. Mutant 3 targets Ser_{112}, replacing a small polar side chain with a bulky, charged side chain (nonpolar residues could not be used because of solubility issues). Because Ser_{112} is the only non-proline residue for which a low rate of saturation transfer was observed in both the early and late phases of aggregation (see Scheme 1), this mutation should not prevent ordered aggregation. Thus, our objective here is to introduce a "disruptive" mutation that is nondisruptive to ordered aggregation.

To understand the impact of these mutations on amyloidogenic interactions, we acquired backbone amide proton STD profiles for each $TTR_{(105-115)}$ variant at regular intervals as it underwent aggregation (Figure 1, left column). AFM images were also acquired at each interval to visualize the consequences of altered interactions on aggregate morphology (Figure 1, right column). Measurements were terminated when random aggregates visibly precipitated or when the sample equilibrated (see the Supporting Information for details). The STD profile for wild-type $TTR_{(105-115)}$ (Figure 1A) is consistent with that reported previously (*12*), with backbone amides near the termini showing a high degree of saturation, and a significant "valley" centered on Leu_{110}. This profile is indicative of early-phase ordered aggregation that will progress to late-phase amyloidogenesis (Figure 1B).

Mutant 1 measurements were terminated at 4 weeks due to equilibration of the sample. Throughout the experiment, the mutant 1 STD profile was broadly similar to that of the wild-type early phase (Figure 1C), except in the immediate vicinity of the mutated residue, suggesting that we had achieved our objective of selectively disrupting interactions associated with late-phase ordered aggregation. Corresponding AFM images revealed the expected result. Protofibrils were observed after aggregation for ~1 week, but these never matured to protofilaments or mature fibrils. The AFM image corresponding to the experiment end point is shown in Figure 1D. A competing process of random aggregation was also apparent, which may be reflected in the STD data as a general "flattening" of the profile (i.e., a smaller difference between the highest and lowest STD value) compared to that of the wild type.

A more detailed comparison of the earliest observed fibrillar aggregates from mutant 1 and wild-type $TTR_{(105-115)}$, shown in Figure 2, reveals substantial differences in supramolecular structure. Protofibrils from mutant 1 are flat, with an average height of 4.0 ± 0.5 Å, suggesting a single-layer, untwisted β-sheet configuration (Figure 2C). This configuration does not appear

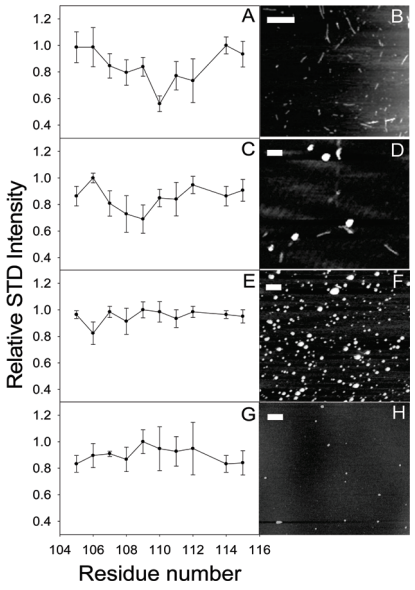

FIGURE 1: Backbone amide proton STD profiles of $TTR_{(105-115)}$ variants (left) with typical AFM images of the corresponding aggregates (right): wild type (A and B), mutant 1 (C and D), mutant 2 (E and F), and mutant 3 (G and H). STD profile error bars are based on data from five replicates. Time points for AFM images shown: (B) 24 h and (D−H) 3 weeks. See the text for details. Scale bars on AFM images are 1 μm (B), 100 nm (D), and 200 nm (F and H).

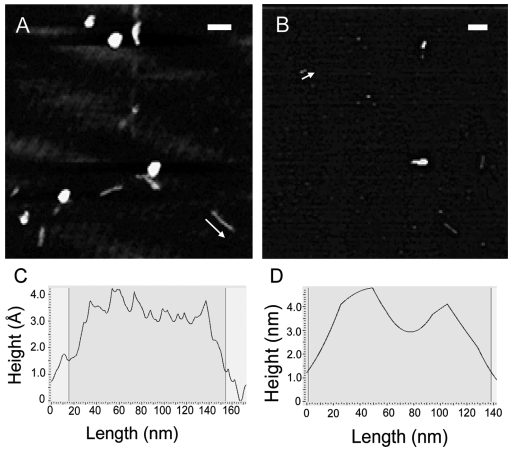

FIGURE 2: Typical supramolecular structures of ordered aggregates of mutant 1 (A and C) and wild-type $TTR_{(105-115)}$ (B and D). AFM image time points: (A) 3 weeks and (B) 6 h. Scale bars are 100 (A) and 300 nm (B). Arrows are adjacent to the protofilaments from which the length−height profiles were acquired and indicate the direction of measurement.

to be stable beyond 120 nm (approximately 300 individual strands), which is consistent with the "breaking" mechanism of nucleated fibril growth introduced by Smith et al. (*20*) in their work on insulin, albeit at a much shorter length. In this case, however, the protofibrils fail to nucleate further growth, giving mutant 1 the unique property of undergoing fully ordered aggregation that stalls at the protofibril stage. We also note that the maximum length of mutant 1 protofibrils corresponds roughly to one full twist in wild-type protofilaments, which may indicate that the instability of longer protofibrils is associated, at least in part, with their untwisted morphology.

Measurements for the earliest observed fibrillar aggregates of wild-type $TTR_{105-115}$ (Figure 2D) give an average height

maximum of 4.5 ± 1.7 nm, which is in agreement with literature values for protofilaments (*19*), and regular protrusions and indents consistent with a twisted structure are present. Thus, sheet−sheet stacking occurs early in the aggregation process, likely before protofibrils reach 120 nm in length.

Experiments involving mutants 2 and 3 were terminated at 4 weeks due to the precipitation of disordered aggregates. The STD profiles of mutants 2 (Figure 1E) and 3 (Figure 1G) were essentially flat, which is indicative of random aggregation. This is confirmed in the corresponding AFM images (Figure 1F,H). Random aggregation (or at least the failure to form fibrillar aggregates under the conditions of the experiment) was the predicted behavior for mutant 2, where the mutation of Ile_{107} was designed to disrupt important interactions in both phases of ordered aggregation. However, failure of mutant 3 to form fibrillar aggregates was unexpected. A number of other mutants were tried, including other mutations of Ser_{112} (see the Supporting Information), but all of these failed to show any degree of ordered aggregation. This result may point to a limitation of the STD approach, which is that it assumes a direct correlation between proximity and the importance of an interaction. It may be that backbone and/or side chain protons on Ser_{112} play an important role in ordered aggregation without being in the (relative) proximity of the fibril on binding. Alternatively, it may be that none of the $TTR_{(105-115)}$ variants assayed were selective enough, resulting in the disruption of important interactions on nearby residues.

In summary, we have manipulated ordered aggregation in a model peptide using a rationale based on an atom-specific map of amyloidogenic interactions. The generation of a $TTR_{(105-115)}$ variant that underwent early processes in ordered aggregation but did not go on to form mature fibrils supports the notion of differing mechanisms in early- and late-stage amyloidogenesis even in "simple" peptide models. This species may also represent a valuable tool for studying early-stage ordered aggregation without interference from late-stage processes. With respect to the $TTR_{(105-115)}$ system specifically, our data strongly support the relevance of side chain interactions at Leu_{110}, specifically sheet−sheet interactions in protofilaments. Failure of variants with "disruptive" mutations at Ser_{112} to form fibrils suggests that this residue may play a role in ordered aggregation in spite of the apparent lack of proximity of its backbone amide or side chain on binding.

ACKNOWLEDGMENT

We thank Xavier Salvatella for help initiating this project and Howard Hunter for technical support in all NMR experiments.

SUPPORTING INFORMATION AVAILABLE

Details of experimental procedures and TOCSY spectra for chemical shift assignments of mutants 1−3. This material is available free of charge via the Internet at http://pubs.acs.org.

REFERENCES

1. Glenner, G. G., and Wong, C. W. (1984) *Biochem. Biophys. Res. Commun. 122*, 1131–1135.
2. Nelson, R., Sawaya, M. R., Balbirnie, M., Madsen, A. O., Riekel, C., Grothe, R., and Eisenberg, D. (2005) *Nature 435*, 773–778.
3. Sunde, M., Serpell, L. C., Bartlam, M., Fraser, P. E., Pepys, M. B., and Blake, C. C. F. (1997) *J. Mol. Biol. 273*, 729–739.
4. Fandrich, M., Fletcher, M. A., and Dobson, C. M. (2001) *Nature 410*, 165–166.
5. Dobson, C. M., Šali, A., and Karplus, M. (1998) *Angew. Chem., Int. Ed. 37*, 868–893.
6. Terry, R. D., Masliah, E., Salmon, D. P., Butters, N., Deteresa, R., Hill, R., Hansen, L. A., and Katzman, R. (1991) *Ann. Neurol. 30*, 572–580.
7. Janson, J., and Butler, P. C. (1997) *Diabetes 46*, 814.
8. Lambert, M. P., Barlow, A. K., Chromy, B. A., Edwards, C., Freed, R., Liosatos, M., Morgan, T. E., Rozovsky, I., Trommer, B., Viola, K. L., Wals, P., Zhang, C., Finch, C. E., Krafft, G. A., and Klein, W. L. (1998) *Proc. Natl. Acad. Sci. U.S.A. 95*, 6448–6453.
9. Carullaa, N., Zhou, M., Arimon, M., Gairi, M., Giralt, E., Robinson, C. V., and Dobson, C. M. (2009) *Proc. Natl. Acad. Sci. U.S.A. 106*, 7828–7833.
10. Li, D. W., Han, L., and Huo, S. H. (2007) *J. Phys. Chem. B 111*, 5425–5433.
11. Campioni, S., Mannini, B., Zampagni, M., Pensalfini, A., Parrini, C., Evangelisti, E., Relini, A., Stefani, M., Dobson, C. M., Cecchi, C., and Chiti, F. (2010) *Nat. Chem. Biol. 6*, 140–147.
12. Liang, Y. F., Jasbi, S. Z., Haftchenary, S., Morin, S., and Wilson, D. J. (2009) *Biophys. Chem. 144*, 1–8.
13. Buxbaum, J. N., and Reixach, N. (2009) *Cell. Mol. Life Sci. 66*, 3095–3101.
14. Gustavsson, A., Engstrom, U., and Westermark, P. (1991) *Biochem. Biophys. Res. Commun. 175*, 1159–1164.
15. Jaroniec, C. P., MacPhee, C. E., Bajaj, V. S., McMahon, M. T., Dobson, C. M., and Griffin, R. G. (2004) *Proc. Natl. Acad. Sci. U.S.A. 101*, 711–716.
16. Deng, W., Cao, A., and Lai, L. (2007) *Biochem. Biophys. Res. Commun. 362*, 689–694.
17. Mesquida, P., Riener, C. K., MacPhee, C. E., and McKendry, R. A. (2007) *J. Mater. Sci.: Mater. Med. 18*, 1325–1331.
18. Paci, E., Gsponer, J., Salvatella, X., and Vendruscolo, M. (2004) *J. Mol. Biol. 340*, 555–569.
19. MacPhee, C. E., and Dobson, C. M. (2000) *J. Mol. Biol. 297*, 1203–1215.
20. Smith, J. F., Knowles, T. P. J., Dobson, C. M., MacPhee, C. E., and Welland, M. E. (2006) *Proc. Natl. Acad. Sci. U.S.A. 103*, 15806–15811.